Diffusional Kurtosis Imaging Assessment of Tuberous Sclerosis Complex

V. Adisetiyo[1], S. S. Milla[2], H. Weiner[3], C. Hu[2], A. Tabesh[2], J. H. Jensen[1,2], and J. A. Helpern[1,2]
[1]Neuroscience and Physiology, New York University School of Medicine, New York, NY, United States, [2]Radiology, New York University School of Medicine, New York, NY, United States, [3]Neurosurgery, New York University School of Medicine, New York, NY, United States

INTRODUCTION:

Tuberous sclerosis complex (TSC) is a rare, multi-system genetic disease that, as a result of dominant mutations of TSC1 and TSC2 genes, causes tumors/lesions to grow in various organs. In the central nervous system, TSC is predominantly characterized by cortical/subcortical tubers which are responsible for the seizures (90%) and mild to severe developmental delays found in TSC [1]. Although tuber lesions are presumed to contribute to epileptogenesis in TSC, a few studies have identified "silent'" tubers with active surrounding perilesion tissue that appear normal on conventional MRI images [2, 3]. In this preliminary study, we aim to quantitatively characterize the in-vivo microstructure of tuber lesions (L) as compared to perilesion (P) tissue and normal appearing contralateral (C) perilesion tissue using metrics derived from Diffusional Kurtosis Imaging (DKI) [4, 5]. To our knowledge, this is the first study to apply DKI in TSC. Investigation of DKI in this cohort provides an additional incentive as there is extensive literature on the histology of resected TSC tuber lesions and perilesion tissue, thus allowing in-vivo DKI metric values to be directly associated with morphological human cell properties in-vitro.

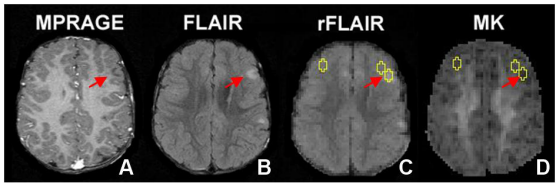

Figure 1. Lesion, Perilesion, Contralateral Perilesion ROIs

METHODS:

This study involved 6 participants with TSC (3 males) with a mean age of 6.03 years (range: 2.23-10.17 years) and 6 age-matched controls (6 males) with a mean age of 6.18 years (range: 2.67-10.22 years). All subjects were recruited from the NYU Langone Medical Center by a pediatric neurosurgeon (HW) and pediatric neuroradiologist (SM) with approval from the NYU IRB. Subjects were either TSC patients that required MRI for clinical purposes or controls who received MRIs for clinical issues not due to significant neurological symptoms and were cleared of any radiologic abnormalities. Imaging was conducted on a 1.5T MR system (Siemens Avanto). Whole brain DKI data were acquired using 30 gradient encoding directions and 3 b-values (0, 1000, 2000 s/mm²). Other parameters include: TR/TE: 4500/96 ms, FOV: 230×230 mm², matrix: 88×88×30, slice thickness: 5 mm, gap: 0%, 1 average, time: 4 min, 48 sec. FLAIR images: TR/TE: 9000/99 ms, FOV: 220×220 mm², matrix: 256×256×30, slice thickness: 5.0 mm. T1-weighted MPRAGE images: TR/TE: 2100/3.79 ms, matrix: 256×256×160, voxels: 1 mm³. Parametric maps for mean kurtosis (MK, range 0-2), axial kurtosis (AK, range 0-2), radial kurtosis (RK, range 0-3), fractional anisotropy (FA, range 0-1), mean diffusivity (MD, range 0-3 $\mu m^2/ms$), axial diffusivity (AD, range 0-3 $\mu m^2/ms$) and radial diffusivity (RD, range 0-3 $\mu m^2/ms$) were calculated using in-house software (Diffusional Kurtosis Estimator) running in Matlab. FLAIR and MPRAGE images were registered and resliced into parametric map space using ART2 [6]. For each subject: 1) FLAIR was registered to the non-diffusion weighted volume (b=0) using a linear rigid-body transformation. The FLAIR in b=0 space was then registered to the b=0 volume using an iterative-linear registration program that corrects for subject motion. These two matrices were multiplied to produce one linear rigid-body transformation. 2) The linear rigid-body warping transformation was then applied to the FLAIR image. 3) Same steps were conducted on the MPRAGE. As done clinically, tuber lesions (L) were identified as distinct hyperintensities in the FLAIR (Figure 1B). An oval region of interest (ROI) was drawn within the identified lesion on the registered FLAIR in one slice where there was normal appearing tissue in the contralateral region (Figure1C). The same ROI was then replicated over the perilesion (P) region adjacent to the hyperintense boundary and over the contralateral (C) region matching the perilesion location to serve as a within subject control. For the control subjects, ROIs were reproduced to anatomically match the L, P, and C ROIs of the TSC subject they were age-matched to. All ROIs within and between subjects had the same shape and area and were sampled from bordering gray and white matter gyral regions. Tissue anatomy was verified by overlaying the ROIs on the registered MPRAGE. ROIs were then applied to all parametric maps to obtain metric means (Figure 1D).

RESULTS and DISCUSSION:

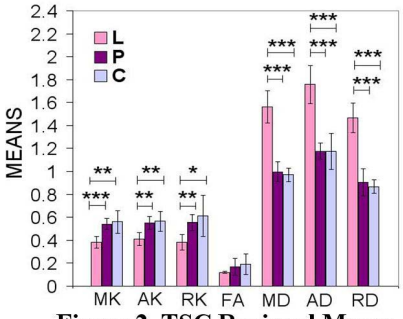

Figure 2. TSC Regional Means

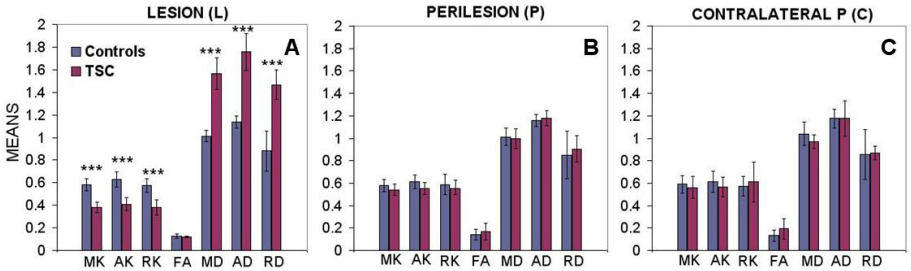

Figure 3. Controls vs. TSC Means

***$p<0.001$, **$p<0.01$, *$p<0.05$

Two-sample t-tests (two-tailed) of regions within the TSC group revealed MK, AK, and RK means for the L to be significantly lower than the means for the P (L vs. P: MK $p<0.001$, AK $p=0.001$, RK $p=0.001$) and C (L vs. C: MK $p=0.003$, AK $p=0.004$, RK $p=0.015$). MD, AD, and RD means for the L were significantly higher than the means for the P (L vs. P: MD $p<0.001$, AD $p<0.001$, RD $p<0.001$) and C (L vs. C: MD $p<0.001$, AD $p<0.001$, RD $p<0.001$). FA means for the L were lower but not significantly different from the P and C means. For all metrics, the P means did not significantly differ from the C means (Figure 2). The MD and FA results are similar to findings of a previous DTI study of TSC [7]. These results suggest that the microstructure of the lesion is compromised equally in radial and axial directions whereas perilesion tissue does not seem to differ from normal appearing contralateral tissue. The TSC and control group did not statistically differ in age ($p=0.94$, two-tailed). Comparison between both groups' L, P and C means also replicate the regional trends within the TSC group and verify that only the lesion differs in microstructure when compared to normal tissue (Figure 3). C means were not significantly different between the TSC and control group thus validating the use of contralateral perilesion tissue as a within subject control (Figure 3C). As expected, the L, P and C means within the control group were not significantly different. Given the very small cohort, interpretation of these results should be made with caution. Nonetheless, these findings suggest that lesions are associated with a substantial increase in diffusivity (as indicated by MD, AD, and RD) and a substantial decrease in diffusional heterogeneity (as indicated by MK, AK, and RK). Future analysis will include more subjects, as well as to compare tuber and perilesion values of TSC patients with and without seizures and correlate the observed diffusional changes with histological observations of abnormal dysplastic neurons.

REFERENCES:

[1] Crino PB, et al. (1999). Neurology. 53(7):1384-90. [2] Madhavan D, et al. (2007) Epilepsy Behav. 11(1):140-6. [3] Major P, et al. (2009). Epilepsia, 50(1):147-54. [4] Jensen JH, et al. (2005). Magn Reson Med. 53(6):1432-40.; [5] Lu H, et al. (2006). NMR Biomed.19(2):236-47. [6] Ardekani BA, et al. (1995). J Comput Assist Tomogr. 19(4):615-23. [7] Karadag D, et al. (2005). Pediatr Radiol. 35:980-3.